Journal of Nano- and Electronic Physics
Vol. **15** No 6, 06005(5pp) (2023)

Журнал нано- та електронної фізики
Том **15** № 6, 06005(5cc) (2023)

Numerical Simulation and Performance Enhancement of CZTS Thin Film Solar Cells

Mohammed Zebach[1,*], Abderrahmane Hemmani[2], Hamid Khachab[3]

Tahri Mohammed University, Laboratory of Development Renewables Energies & Their Application in Saharan Areas, 08000 Bechr, Algeria

(Received 23 September 2023; revised manuscript received 17 December 2023; published online 27 December 2023)

The development of thin-film solar cells allows researchers to evaluate different materials in order to improve the efficiency of cell conversion. This is particularly relevant for the third generation of solar photovoltaic cells, which incorporate layer materials at the nano- and micrometre-scale, avoiding non-toxic and earth-abundant materials with reduced manufacturing costs. In recent years, scientists have focused their studies on the lowest-cost and most stable materials, such as kesterite, based on the following elements: copper, zinc, tin, and sulfur (CZTS). It's one of the most efficient absorbing material layers in thin-film solar cells, with a direct bandgap (1.38-2.0 eV) and a high absorption coefficient (~ 10^4 cm^{-1}). CZTS has tremendous potential due to its earth abundance, non-toxicity, and low production costs compared to other thin film materials. However, several challenges still exist regarding the control of secondary phases, compositional homogeneity, electronic defects, and instability issues during fabrication that limit the efficiency of CZTS-based solar cells and have yet to be overcome. In this paper, we implement a mathematical model of a heterojunction CdS-CZTS thin film solar cell. Hence, the output performance of solar cells can be evaluated by varying the material, parameters, dimensional ratios, and other variables in the cells; essentially,the conversion efficiency is given at a value of $\eta = 12.79$ % results of simulations using Matlab Simulink software. The improved conversion efficiency obtained through our simulation study falls within the range of experimental values achieved for this type of thin film solar cell design, as demonstrated by the laboratory's record measured efficiency of around 12.6 % for a similar heterojunction cell based on CZTS reported by Wei Wang et al., while the theoretical maximum conversion efficiency for an ideal CZTS-based solar cell is estimated at 32.4 % according to the Shockley Queisser limit. As our simulated efficiency value is close to measured experimental values while still significantly below the theoretical limit, this suggests that further efficiency improvements may still be achievable through material property and cell design optimizations.

Keywords: CZTS solar cells, Simulation, Thin film, Heterojunction, Matlab.

DOI: 10.21272/jnep.15(6).06005 PACS numbers: 07.05.Pj, 07.05.Wr, 68.55.Nq

1. INTRODUCTION

With exponential population growth, conventional energy use has increased at a remarkable rate. This huge energy demand is mainly met by fossil fuels. However, these fossil fuels are limited resources[1]. 80 % of energy is generated from these resources e.g. oil, gas, coal, etc. and the remaining 20 % of energy is from renewable energy sources e.g. water, solar, wind, etc[2]. Solar energy is easily available, directly accessible, and a free source of energy on Earth, and it is free of charge. The solar insolation on the earth is incident directly approximately 1.2×10^5 TW [3]. Solar cell technology has attracted the attention of researchers. About 80 % of the current photovoltaic market is based on single-crystalline (*c*-Si) and multi-crystalline (*mc*-Si) wafers called first generation[4]. Silicon-based solar cell technology is based on an absorbent material with an indirect band gap, thereby requiring a thick layer to absorb most of the incident solar radiation, contributing to the higher cost of PV devices. Hence, recent PV developers have tended to focus on thin film PV technologies called second generation are based on direct band gap materials, which correspond to a high absorption coefficient between 10^4 and 10^5 cm^{-1} and therefore, a thickness of 1-5 μm being generally able to absorb most of the solar radiation [5]. The most commonly used thin film materials are, amorphous silicon (*a*-Si) has an efficiency of 10.2 % ± 0.5, While cadmium Telluride (CdTe) thin films have provided record power conversion efficiencies of 21.5 % [6]. Copper indium gallium diselenide (CIGS)-based cells have recently reached a record conversion efficiency of 21.7 % [7]. Despite this performance, the development of these materials has been interrupted due, on one hand, to the toxicity of cadmium (Cd) and its membership in the heavy metal family and the lack of Telluride (Te) and the high cost of indium (In) and gallium (Ga) [8-9]. Therefore, researchers have explored other ways of using eco-friendly materials with earth-abundant elements, Earth-abundant, nontoxic kesterite CZTS material is a promising absorber for thin-film photovoltaics. Its physical and photovoltaic properties, such as its high absorption coefficient (> 10^4 cm^{-1}), tunable bandgap (1.0-1.5 eV), and a high theoretical conversion efficiency of 32 % according to the Shockley Queisser limit [10], CZTSSe based on molybdenum substrate demonstrated a record cell efficiency of around 12.6 % via a hydrazine pure-solution process [8].

2. NUMERICAL STUDY

The numerical method allows us to model and simulate CZTS thin film solar cells with different software by exceeding laboratory experimental values Where Wei Wang et al demonstrated a record cell efficiency of around 12.6 % and approaching the theoretical conversion efficiency of 32.4 % according to the Shockley Queisser limit.

* zebach.mohammed@univ-bechar.dz

Table 1 – Output performance of the numerical simulation CZTS thin film solar cell by different softwares

Year	η (%)	$J_{sc}\left(\frac{mA}{cm^2}\right)$	V_{OC} (mV)	FF(%)	soft-ware	Ref
2012	13.41	19.31	1.002	69.35	SCAPS-1D	[11]
2015	15.68	19.99	0.956	82.1	AMPS-1D	[12]
2016	12.1	19.2	0.83	76.06	Matlab	[5]
2016	14.57	18.68	1.009	77.29	SCAPS-1D	[13]
2017	18.05	25.67	1.02	69.26	SCAPS-1D	[14]
2019	12.26	18.73	0.97	67.32	SCAPS-1D	[15]
2019	13	19.3	0.836	76.1	Matlab	[16]
2021	24.50	47.73	0.63	80.73	SCAPS-1D	[17]

In this paper, our simulation carried out by the MATLAB programming language shows the accuracy in solving mathematical equations, the resolution of the continuity equation combined with Poisson's equation, and the current density that are needed in a mathematical model of a CdS-CZTS thin film solar cell.

3. SIMULATION MODEL

3.1 Cell Structure

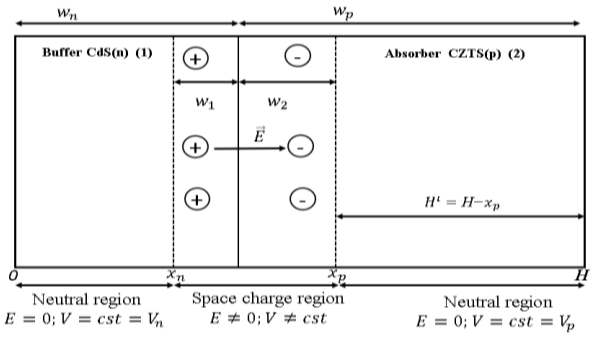

Fig. 1 – Dimensions and structure of thickens CdS/CZTS heterojunction thin-film solar cell

$$w_1 = \left(\frac{2N_a}{eN_d}\frac{\varepsilon_1\varepsilon_2}{\varepsilon_1 N_d + \varepsilon_2 N_a}\right)^{\frac{1}{2}}(V_d)^{\frac{1}{2}} \quad (1)$$

$$w_2 = \left(\frac{2N_d}{eN_a}\frac{\varepsilon_1\varepsilon_2}{\varepsilon_1 N_d + \varepsilon_2 N_a}\right)^{\frac{1}{2}}(V_d)^{\frac{1}{2}} \quad (2)$$

H' is the thickness of the neutral charge zone of the P layer and : $x_n = w_n - w_1$; $x_p = x_n + w_1 + w_2$; $H = w_n + w_p$; $H' = H - x_p = w_p - w_2$, ε_1 and $\varepsilon_2$is the permittivity of the buffer and absorber layer (CZTS) respectively, where V_d is the diffusion potential given by[18]:

$$V_d = \frac{1}{q}\left[E_{g2} + (\chi_2 - \chi_1)\right] + U_q \ln\left(\frac{N_a N_d}{N_{C1} N_{V2}}\right) \quad (3)$$

where $\chi_1$and χ_2 are the electronic affinities of the absorbent and buffer layers, respectively, $U_{\mathbf{q}} = \frac{KT}{q} \approx 26\text{mV}$ is the thermodynamic potential, N_a and N_d are acceptors and donors concentrations, respectively, N_{C1} is the effective conduction band density of the states, N_{V2} is the effective valence band density of the states, and E_{g2} is the CZTS band gap.

3.2 Optical Properties

Figure 2 shows the variation of photon flux in the Sun's spectrum concerning both wavelength and photon energy. The photon flux shows a gradual decrease with increasing wavelength.

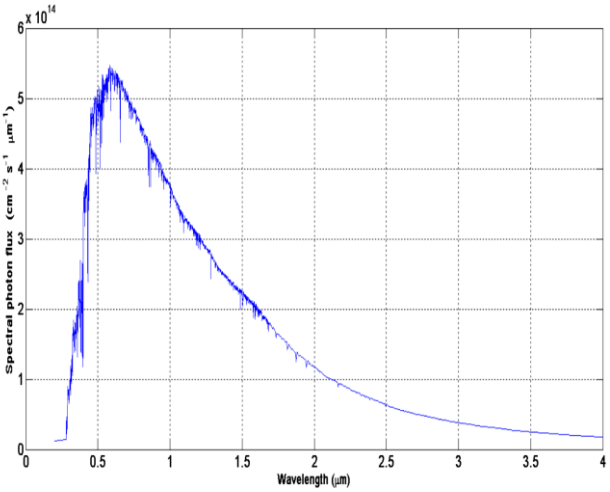

Fig. 2 – Variation of photon flux of Sun's spectrumAM1.5 as a function of wavelength and photon energy

The absorption coefficient $\alpha(\lambda)$ for the two materials CZTS and CdS are given by [19] and [20] respectively:

$$\alpha_{\text{CdS}}(\lambda) = \frac{A}{E}\left(E - E_{gCdS}\right)^{\frac{1}{2}} \quad (4)$$

$$\alpha_{\text{CZTS}}(\lambda) = B\left(E - E_{gCZTS}\right)^{\frac{1}{2}} \quad (5)$$

Where: $A = 3.224 \times 10^4\ \text{cm}^{-1}\text{eV}^{\frac{1}{2}}$ and $B = 2 \times 10^4\ \text{cm}^{-1}\text{eV}^{\frac{1}{2}}$ are constants, E is the photon energy $E = h\nu = \frac{hc}{\lambda}$ and $E_{gCdS} = 2.4\ ev$ and $E_{gCZTS} = 1.5\ ev$ are the bandgaps of CdS and CZTS respectively.

It is clear from Figure 3 and Figure 4, which represent the absorption coefficient as a function of wavelength, Results of calculation using Matlab software which give us values similar to previous research values that state that a high absorption coefficient for CZTS ($> 10^4\ \text{cm}^{-1}$). And on it, we confirm the CZTS absorbs more photons than CdS $E_{g\text{CZTS}} > E_{g\text{CdS}}$.

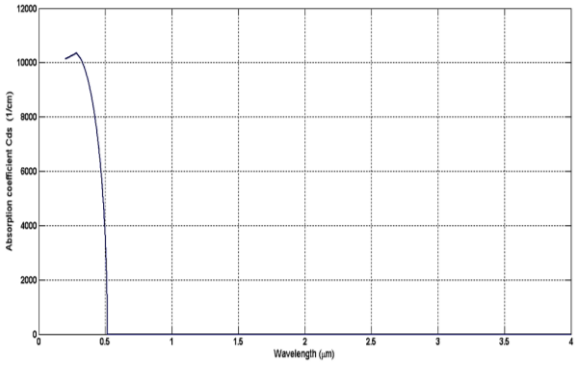

Fig. 3 – Absorption coefficient of the CdS as a function of the wavelength

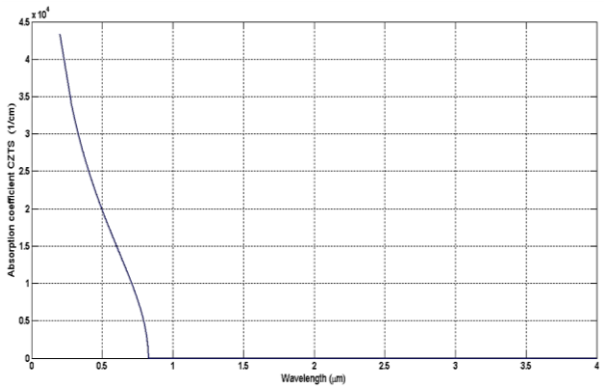

Fig. 4 – Absorption coefficient of the CdS as a function of the wavelength

3.3 Photocurrent Density

In the three regions, the resolution of the continuity equation in combination with the Poisson equation and the current density equation allows us to calculate the current density in each of these three regions. The total photocurrent density $\boldsymbol{J_{ph}}$ is the integral of the photocurrent to a particular Wavelength $\boldsymbol{J_{ph}(\lambda)}$ over the entire solar spectrum, where λmin and λmax are 0.2 μm and 4 μm, respectively.

$$J_{ph}(\Lambda) = J_n(\Lambda) + J_p(\Lambda) + J_{zce}(\Lambda) \tag{6}$$

$$J_{ph} = \int_{\lambda\mathrm{MIN}}^{\lambda\mathrm{MAX}} J_{ph}(\lambda)d\lambda = \int_{\lambda\mathrm{MIN}}^{\lambda\mathrm{MAX}} (J_p(\lambda) + J_n(\lambda) + J_{zce}(\lambda))d\lambda \tag{7}$$

Taking into account the phenomenon of generation presented by the rate $\boldsymbol{G(\lambda, x)}$ given by:

$$\mathrm{G}(\lambda,\mathrm{x}) = \alpha(\lambda)\phi(\lambda)(1-\mathrm{R}(\lambda)).\mathrm{e}^{(\lambda).x}) \tag{8}$$

Where R is the reflectivity.

In the first neutral zone, N (CdS), the electric field $\mathbf{E = 0}$ and minorities are holes, given by:

$$J_p = -qD_p\left(\frac{dp_n}{dx}\right)_{x_n} = \left[\frac{q\phi(\lambda)(1-R(\lambda))\alpha_1 L_p}{(\alpha_1^2 L_p^2 - 1)}\right] \times \times \left[\frac{\left(\frac{S_P L_P}{D_p} + \alpha_1 L_p\right) - e^{-\alpha_1 x_n}\left(\frac{S_P L_P}{D_p} cosh\frac{x_n}{L_p} + sinh\frac{x_n}{L_p}\right)}{\frac{S_P L_P}{D_p} sin\,h\left(\frac{x_n}{L_p}\right) + cosh\left(\frac{x_n}{L_p}\right)} - \alpha_1 L_p e^{-\alpha_1 x_n}\right] \tag{9}$$

Where: $L_p = \left(D_p \cdot \tau_p\right)^{\frac{1}{2}}$; $\alpha_{\mathrm{CdS}}(\lambda) = \alpha_1$;$p_n$hole concentration in the N region and $D_p = U_q \cdot \mu_p$ are holes' diffusion length and diffusion coefficient respectively. S_P is the hole recombination velocity at CdS front surface.

In the second neutral zone P (CZTS), the electric field $E = 0$ and minorities are electrons, given by:

$$\boldsymbol{J_n = qD_n\left(\frac{dn_p}{dx}\right)_{x_{j+(w_1+w_2)}} = \frac{q\phi(\lambda)(1-R(\lambda))\,L_n}{\alpha_2^2 L_n^2 - 1}\exp\left(-\alpha_1\left(x_j + w_1\right) - \alpha_2 w_2\right) \times \left[\alpha_2 L_n - \frac{\frac{S_n L_n}{Dn}\left(cosh\left(\frac{H'}{Ln}\right)exp(-\alpha_2 H')\right) + sinh\left(\frac{H'}{Ln}\right) + \alpha_2 L_n\, exp(-\alpha_2 H')}{\frac{S_n L_n}{Dn} sinh\left(\frac{H'}{Ln}\right) + cosh\left(\frac{H'}{Ln}\right)}\right)} \tag{10}$$

Where: $L_n = (D_n \cdot \tau_n)^{\frac{1}{2}}$; $\alpha_{\mathrm{CZTS}}(\lambda) = \alpha_2$; n_p *the* concentration of electrons in the P region and $D_n = U_q \cdot \mu_n$ are electrons diffusion length and diffusion coefficient respectively. S_n is the electron recombination velocity at the CZTS back surface. In the space charge region (Depletion region), the electric field $\mathrm{E} \neq 0$, given by:

$$J_{zce} = q\phi(\lambda)\left(1 - R(\lambda)\right)e^{-\alpha_1 x_n}[(1 - e^{-\alpha_1 w_1}) + e^{-\alpha_1 w_1}(1 - e^{-\alpha_2 w_2})] \tag{11}$$

3.4 Solar Cell Characteristics

The current-voltage J-V characteristic of the cell is given by the following equation:

$$J = J_{ph} - J_0\left(e^{\frac{V+R_sJ}{QU_q}} - 1\right) - \frac{V+R_sJ}{R_{sh}} \tag{12}$$

$\boldsymbol{J_0}$ saturation current density; Q diode ideality factor; R_s and R_{sh} series and parallel resistances.

The numerical solution of equation J-V for $V = 0$ and $J = 0$ gives respectively as a solution the short-circuit current density $J = J_{sc} = J_{ph}$ and the open circuit voltage $V = Vco$.

The maximum power, P_m can be calculated by:

$$P_m = (J.V)_{\max} \tag{13}$$

And therefore, we can calculate the fill factor and the conversion efficiency which are respectively given by

$$FF = \frac{P_m}{J_{sc}V_{co}} \tag{14}$$

$$\eta = \frac{P_m}{P_i} \tag{15}$$

$P_i = 100\ \mathrm{mW - cm^{-2}}$ is the incident power in standard conditions AM1.5G.

Table 2 – Parameters of the CdS/CZTS cell used during the simulation

Layer properties	**CdS**	**CZTS**	**Ref**
Layer thickness w(nm)	50	3000	[11][21]
Electron affinity, χ(eV)	4.2	4.1	[22]
Relative permittivity, ε_r	10	13.6	[21][22]
Electron mobility, $\mu_n\left(\frac{\mathrm{cm}^2}{\mathrm{V}}.\mathrm{s}\right)$	100	100	[23]
Hole mobility, $\mu_p\left(\frac{\mathrm{cm}^2}{\mathrm{V}}.\mathrm{s}\right)$	25	25	[24]
Donor concentration $(\mathrm{cm}^{-3})N_d$	1×10^{18}	–	[24]
Acceptor concentration $(\mathrm{cm}^{-3})N_a$	–	1×10^{17}	[24]
Band gap energy E_g(eV), base parameter	2.4	1.5	[21]
Effective conduction band density of states, $N_{\mathrm{C}}(\mathrm{cm}^{-3})$	2.2×10^{18}	2.2×10^{18}	[22]

Effective valence band density of states, $N_V(\text{cm}^{-3})$	1.8×10^{19}	1.8×10^{19}	[22]
Hole recombination velocity at CdS front surface, $S_p\left(\frac{\text{cm}}{\text{s}}\right)$	10^7	–	[24]
Electron recombination velocity at CZTS back surface, $S_n\left(\frac{\text{cm}}{\text{s}}\right)$	–	10^7	[24]
Defect density, $N_t(\text{cm}^{-3})$	1×10^{17}	1.35×10^{15}	[25]
Electron capture cross section, $\sigma_e(\text{cm}^2)$	10^{-17}	10^{-14}	[48]
Hole capture cross section, $\sigma_h(\text{cm}^2)$	10^{-13}	10^{-14}	[25]
General device properties			
Reflectivity, R	0.1		[26]
Series resistance, $R_S(\Omega - \text{cm}^2)$	0.72		[27]
Diode ideality factor Q	1.45		
Cell temperature, $T(K)$	300		

4. RESULTS AND DISCUSSION

Depending on the simulation using the CdS/CZTS parameters in Table 2, we first had to determine the current densities due to carriers generated in the two neutral regions N (CdS) and P(CZTS) as well as in the space charge region. In these three regions, the resolution of the continuity equation is in combination with the Poisson equation and current density equations. Indeed, the calculation of this photocurrent permit to determine the electrical characteristics of the photovoltaic thin film solar cell (CdS/CZTS) and to plot the characteristics J(V) and P(V) that shown in Figures 4 and 6.

Table 3 show the output performance of heterojunction CdS/CZTS cell, characterized mainly by open circuit voltage $\boldsymbol{V_{oc}}$,short circuit current $\boldsymbol{J_{sc}}$,conversion efficiency $\boldsymbol{\eta}$ and form factor $\boldsymbol{FF}$.

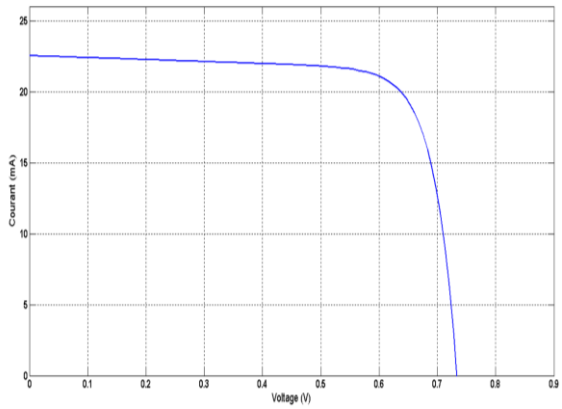

Fig. 5 – The output characteristic $J(V)$ courant-voltage of the CdS/CZTS thin film solar cell

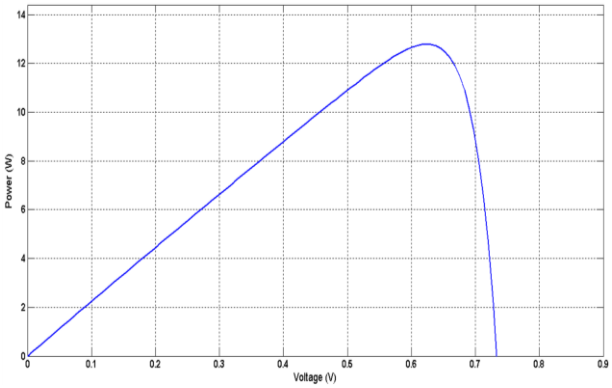

Fig. 6 – The output characteristic $P(V)$ power-voltage of the CdS/CZTS thin film solar cell

Table 3 – The output performance of heterojunction CdS/CZTS simulation

V_{oc}	$J_{ph} \approx J_{sc}$	η	FF
0.735 V	22.5 mA	12.79 %	77.33 %

4.1 Spectral Response

The spectral response in Figure 7 is defined as the ratio between the number of electrons collected and the quantity of photons incident at each wavelength (λ). From 0.2 to 0.4 μm, the quantum efficiency corresponds to the solar spectrum adapted to the CdS buffer layer. And are also caused by the absorption of photons in this layer with the recombination of holes recombinant velocity $S_p = \frac{10^7 \text{cm}}{\text{s}}$ In the second part, from 0.52 to 0.83 μm the quantum efficiency corresponds to the solar spectrum adapted to the CZTS absorber layer, showing the absorption of photons in this layer with recombination of electrons at recombinant velocity $S_n = \frac{10^7 \text{cm}}{\text{s}}$, for a value of 3 μm thickness for the CZTS layer and E_g = 1.5 eV.

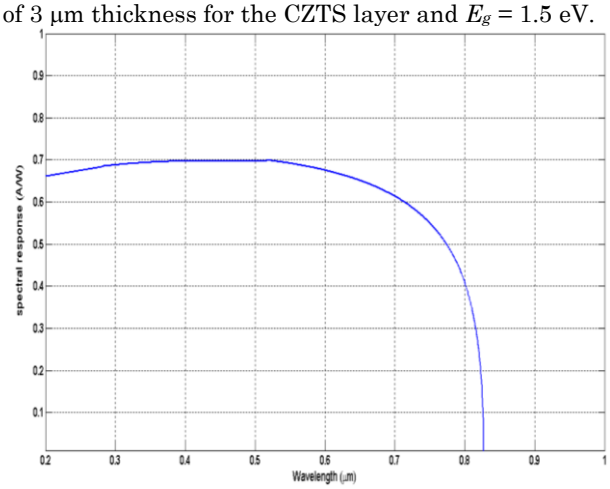

Fig. 7 – Spectral response of a CdS/CZTS thin film solar cell

5. CONCLUSION

The aim of this paper conducted a comprehensive simulation of the heterojunction CdS(n)/CZTS(p) structure. the objective was to analyze the current densities generated within the neutral regions (n and p) and the space charge region, including the parameters of each

material, through the application of the continuity equation combined with Poisson's equation. The derived photocurrent density played a crucial role in uncovering crucial insights regarding the solar cell's $J(V)$ and $P(V)$ characteristics curves and output performance, such as, J_{sc},V_{oc}, FF, η. These findings contribute significantly to the understanding and optimization of the performance of CZTS thin film solar cells.

REFERENCES

1. Xiangbo Song, Xu Ji, Ming Li, Weidong Lin, Xi Luo, Hua Zhang, *Int. J. Photoenergy* **2014**, 613173 (2014).
2. J.J. Scragg, D.M. Berg, P.J. Dale, *J. Electroanal. Chem.* **646**, 52 (2010).
3. A. Muratoglu, M.I. Yuce, *International Journal of Scientific and Technological Research* **1** No 7, 10 (2015).
4. G.L. Agawane, Seung Wook Shin, Min Sung Kim, M.P. Suryawanshi, K.V. Gurav, A.V. Moholkar, Jeong Yong Lee, Jae Ho Yun, P.S. Patil, Jin Hyeok Kim, *Curr. Appl. Phys.* **13** No 5, 850 (2013).
5. A. Benmir, M.S. Aida, *Superlattice. Microstruct.* **91**, 70 (2016).
6. Martin A. Green, Yoshihiro Hishikawa, Ewan D. Dunlop, Dean H. Levi, Jochen Hohl-Ebinger, Anita W.Y. Ho-Baillie, *Prog. Photovoltaics Res. Appl.* **26**, 3 (2018).
7. T. Kato, et al., *IEEE J. Photovoltaics* **7** No 6, 1773 (2017).
8. K.J. Yang, et al., *J. Mater. Chem. A* **4**, 10151 (2016).
9. S.I. Swati, et al., *J. Phys. Conf. Ser.* **1086**, 012010 (2018).
10. W. Shockley, H. J. Queisser, *J. Appl. Phys.* **32**, 510 (1961).
11. A. Haddout, A. Raidou, M. Fahoume, *Appl. Phys. A* **125**, 124 (2019).
12. H. Katagiri, et al., *Sol. Energy Mater. Sol. C.* **49**, 407 (1997).
13. H. Katagiri et al., *Sol. Energy Mater. Sol. C.* **65**, 141 (2001).
14. H. Katagiri, et al., *Proceedings of the 3rd World Conference on Photovoltaic Energy Conversion* (2003).
15. T. Kobayashi, et al., *Jpn. J. Appl. Phys.* **44**, 783 (2005).
16. K. Moriya, K. Tanaka, H. Uchiki, *Jpn. J. Appl. Phys.* **46**, 5780 (2007).
17. H. Katagiri, et al., *Appl. Phys. Express* **1**, 0412011 (2008).
18. A. Ennaoui, et al., *Thin Solid Films* **517**, 2511 (2009).
19. K. Wang, et al., *Appl. Phys. Lett.* **97**, 143508 (2010).
20. K. Tanaka, et al., *Sol. Energy Mater. Sol. C.* **95**, 838 (2011).
21. K. Maeda, et al., *Sol. Energy Mater. Sol. C.* **95**, 2855 (2011).
22. R.B.V. Chalapathy, G.S. Jung, B.T. Ahn, *Sol. Energy Mater. Sol. C.* **95**, 3216 (2011).
23. B. Shin, et al., *Prog. Photovoltaics Res. Appl.* **21**, 72 (2013).
24. S. Ahmed, et al., *Adv. Energy Mater.* **2**, 253 (2012).
25. T. Fukano, S. Tajima, T. Ito, *Appl. Phys. Express* **6**, 062301 (2013).
26. A. Emrani, P. Vasekar, C.R. Westgate, *Sol. Energy* **98**, 335 (2013).
27. T.P. Dhakal, et al., *Sol. Energy* **100**, 23 (2014).

Чисельне моделювання та підвищення продуктивності тонкоплівкових сонячних елементів CZTS

Mohammed Zebach[1], Abderrahmane Hemmani[2], Hamid Khachab[3]

Tahri Mohammed University, Laboratory of Development Renewables Energies & Their Application in Saharan Areas, 08000 Bechr, Algeria

Розробка тонкоплівкових сонячних елементів дозволяє дослідникам оцінювати різні матеріали з метою підвищення ефективності перетворення елементів. Це особливо актуально для третього покоління сонячних фотоелектричних елементів, які включають шарові матеріали в нано- та мікрометровому масштабі, уникаючи нетоксичних і поширених у землі матеріалів із зниженими витратами на виробництво. В останні роки вчені зосередили свої дослідження на найдешевших і найстабільніших матеріалах, таких як кестерит, на основі таких елементів: мідь, цинк, олово і сірка (CZTS). Це один із найефективніших шарів поглинаючого матеріалу в тонкоплівкових сонячних елементах із прямою забороненою зоною (1,38-2,0 еВ) і високим коефіцієнтом поглинання (~ 10^4 $см^{-1}$). CZTS має величезний потенціал завдяки великій кількості землі, нетоксичності та низькій вартості виробництва порівняно з іншими тонкоплівковими матеріалами. Проте все ще існує кілька проблем щодо контролю вторинних фаз, композиційної однорідності, електронних дефектів і проблем нестабільності під час виготовлення, які обмежують ефективність сонячних елементів на основі CZTS і які ще потрібно подолати. У цій статті ми реалізуємо математичну модель гетеропереходу CdS-CZTS тонкоплівкового сонячного елемента. Отже, продуктивність сонячних елементів можна оцінити, змінюючи матеріал, параметри, співвідношення розмірів та інші змінні в елементах. По суті, ефективність перетворення наведена на рівні η = 12,79 % результатів моделювання з використанням програмного забезпечення Matlab Simulink. Покращена ефективність перетворення, отримана завдяки нашому дослідженню моделювання, входить у діапазон експериментальних значень, досягнутих для цього типу дизайну тонкоплівкових сонячних елементів, як продемонстровано рекордно виміряною лабораторією ефективністю приблизно 12,6 % для подібної гетероперехідної клітини на основі звіту CZTS за редакцією Wei Wang та ін., тоді як теоретична максимальна ефективність перетворення для ідеальної сонячної батареї на основі CZTS оцінюється в 32,4 % відповідно до обмеження Шоклі Квейссера. Оскільки наше змодельоване значення ефективності наближається до виміряних експериментальних значень, але все ще значно нижче теоретичної межі, це свідчить про те, що подальше підвищення ефективності все ще може бути досягнуте шляхом оптимізації властивостей матеріалу та конструкції комірки.

Ключові слова: Сонячні елементи CZTS, Моделювання, Тонка плівка, Гетероперехід, Matlab.